## ORIGINAL RESEARCH

CD73 Maintains Hepatocyte Metabolic Integrity and Mouse Liver Homeostasis in a Sex-Dependent Manner

Karel P. Alcedo,[1] Morgan A. Rouse,[1] Gloria S. Jung,[1] Dong Fu,[1] Marquet Minor,[1] Helen H. Willcockson,[1] Kevin G. Greene,[2] and Natasha T. Snider[1]

[1]Department of Cell Biology and Physiology, [2]Department of Pathology and Laboratory Medicine, University of North Carolina at Chapel Hill, Chapel Hill, North Carolina
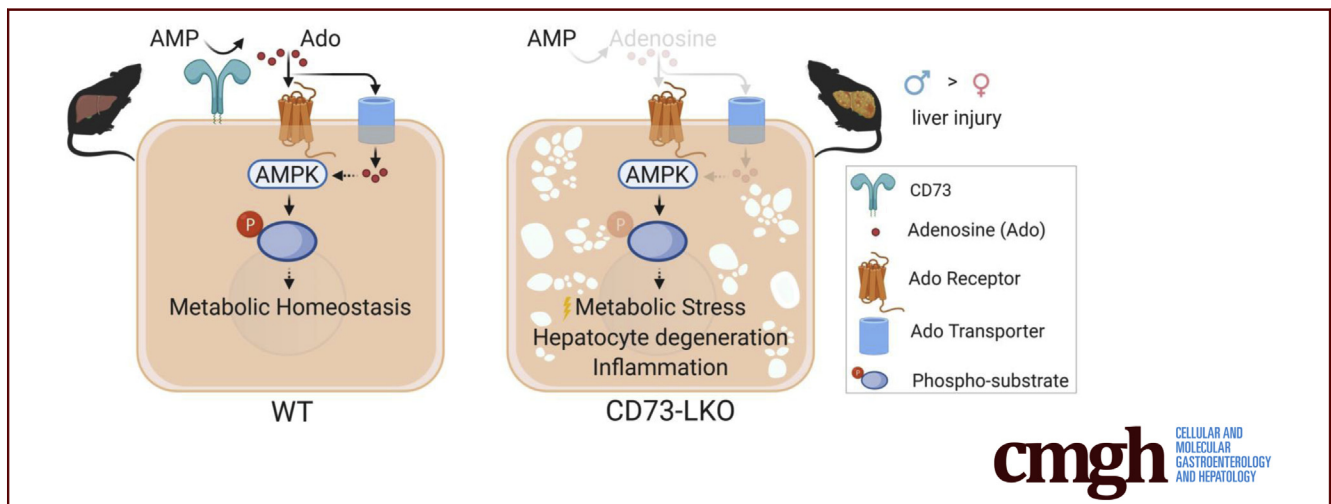
SUMMARY

We developed a new mouse model that showed that CD73, the major extracellular adenosine-producing enzyme, supports long-term liver homeostasis. These results advance our understanding of human disease and therapeutics because CD73 is down-regulated in chronic liver diseases and CD73 inhibitors are in clinical trials for cancer and coronavirus disease 2019.

BACKGROUND & AIMS: Metabolic imbalance and inflammation are common features of chronic liver diseases. Molecular factors controlling these mechanisms represent potential therapeutic targets. CD73 is the major enzyme that dephosphorylates extracellular adenosine monophosphate (AMP) to form the anti-inflammatory adenosine. CD73 is expressed on pericentral hepatocytes, which are important for long-term liver homeostasis. We aimed to determine if CD73 has nonredundant hepatoprotective functions.

METHODS: Liver-specific CD73 knockout (CD73-LKO) mice were generated by targeting the *Nt5e* gene in hepatocytes. The CD73-LKO mice and hepatocytes were characterized using multiple approaches.

RESULTS: Deletion of hepatocyte *Nt5e* resulted in an approximately 70% reduction in total liver CD73 protein ($P < .0001$). Male and female CD73-LKO mice developed normally during the first 21 weeks without significant liver phenotypes. Between 21 and 42 weeks, the CD73-LKO mice developed spontaneous-onset liver disease, with significant severity in male mice. Middle-aged male CD73-LKO mice showed hepatocyte swelling and ballooning ($P < .05$), inflammation ($P < .01$), and variable steatosis. Female CD73-LKO mice had lower serum albumin levels ($P < .05$) and increased inflammatory genes ($P < .01$), but did not show the spectrum of histopathologic changes in male mice, potentially owing to compensatory induction of adenosine receptors. Serum analysis and proteomic profiling of hepatocytes from male CD73-LKO mice showed significant metabolic imbalance, with increased blood urea nitrogen ($P < .0001$) and impairments in major metabolic pathways, including oxidative phosphorylation and AMP-activated protein kinase (AMPK) signaling. There was significant hypophosphorylation of AMPK substrates in CD73-LKO livers ($P < .0001$), while in isolated hepatocytes treated with AMP, soluble CD73 induced AMPK activation ($P < .001$).

CONCLUSIONS: Hepatocyte CD73 supports long-term metabolic liver homeostasis through AMPK in a sex-dependent manner. These findings have implications for human liver diseases marked by CD73 dysregulation. *(Cell Mol Gastroenterol Hepatol 2021;12:141–157; https://doi.org/10.1016/j.jcmgh.2021.01.016)*

Keywords: Adenosine; Inflammation; AMP-Activated Protein Kinase; Ecto-5'-Nucleotidase; Hepatic Zonation..

The highly integrated metabolic activities of hepatocytes control physiological homeostasis and are perturbed in chronic liver diseases. Nonalcoholic fatty liver disease (NAFLD) is the most prevalent chronic liver disease in children and adults, and a major risk factor for the development of cirrhosis and hepatocellular carcinoma (HCC).[1,2] A lack of approved therapies renders NAFLD a major health problem, estimated to affect 25% of the global population, including 80 million people in the United States.[3] In recognition that NAFLD is principally a metabolic disease, a new nomenclature was proposed: metabolic-associated fatty liver disease.[4] From that standpoint, understanding how hepatocytes maintain long-term energy homeostasis will be critical for addressing the key mechanisms behind this complex and heterogeneous disorder.

It was shown more than 50 years ago that adenosine triphosphate (ATP) injections increase hepatic ATP content and can prevent the development of fatty liver in rodents.[5] Moreover, patients with nonalcoholic steatohepatitis, the most severe form of NAFLD, have significantly impaired capacity for replenishing hepatic ATP stores after transient depletion.[6] Numerous biochemical reactions control ATP metabolism and utilization by hepatocytes, including the enzymatic hydrolysis of extracellular ATP to form adenosine monophosphate (AMP), which is metabolized further to adenosine by ecto-5'-nucleotidase (CD73).[7] Adenosine regulates many physiological responses via activation of adenosine receptors,[8] and it also can be taken up inside the cell via specific transporters[9] and phosphorylated back to AMP by adenosine kinase.[10] A major function of adenosine is to reduce metabolic demand and conserve energy, but it is not known what role CD73 plays in this process, despite being the major extracellular adenosine regulator across different tissues and cell types.[11,12] Insights into CD73 mechanisms have particular relevance to liver biology and disease because the messenger RNA (mRNA) expression and enzymatic activity of CD73 are downregulated significantly in human NAFLD, cirrhosis, and HCC via transcriptional,[13] post-transcriptional,[14] and post-translational[15] mechanisms. The latter 2 mechanisms involve production of a catalytically deficient splice variant (CD73S) and catalytically impaired high-mannose glycosylation variant.[12]

Although CD73 has ubiquitous expression,[12] recent single-cell profiling experiments have shown that its mRNA is zonally distributed in epithelial tissues, including the liver,[16] intestine,[17] and kidney.[18] CD73 is induced transcriptionally by hypoxia[19] and CD73-generated adenosine directly protects multiple epithelial tissues, including the liver, against hypoxic injury.[20–22] Previous studies have shown an allostatic function for CD73 in response to severe oxygen deprivation, but presently it is not known if CD73 functions in the long-term maintenance of liver homeostasis. Addressing this question is important because oxygen tension across the hepatic lobule is a key determinant of physiological metabolic zonation.[23] Metabolic zonation refers to the heterogeneous distribution of enzyme activities, resulting in periportal predominance of protein secretion, cholesterol synthesis, fatty acid oxidation, and ureagenesis, and pericentral predominance of glycolysis, lipogenesis, and bile acid synthesis. This structured division of labor among healthy hepatocytes is disrupted in chronic liver diseases such as NAFLD.[24]

Given the earlier-described observations, and the known functions of adenosine in regulating hepatic glucose and lipid metabolism,[25] we hypothesized that CD73 has nonredundant homeostatic functions in the liver. To test this hypothesis, we generated mice with a targeted deletion of the CD73-encoding gene Nt5e in hepatocytes and characterized their liver phenotypes using multiple approaches. Our findings showed unanticipated age- and sex-dependent functions of CD73 in the long-term maintenance of hepatocyte metabolism and liver homeostasis. As such, these results add a cellular-level understanding of this key enzyme, in particular its relatively underappreciated functions in epithelial tissues. Importantly, these findings have translational implications for human liver diseases, as well as anti-CD73 antibodies and inhibitors, which currently are undergoing clinical development for cancer[26] and COVID-19 immunotherapy.[27]

Results

Pericentral Hepatocytes Account for the Bulk of CD73 Expressed in the Normal Mouse Liver

Using single-cell RNA transcriptomic data from the Tabula Muris project,[28] we compared Nt5e expression across different cell types in the mouse liver. Both fluorescence-activated cell–sorted and microfluidic droplet-captured cells showed that hepatocytes are the primary cell types expressing Nt5e (Figure 1A–D). Approximately 30% of hepatocytes, 7% of leukocytes and natural killer cells, and <2% of Kupffer cells and liver sinusoidal endothelial cells express Nt5e, while cholangiocytes and B cells lack Nt5e expression (Figure 1A–D). To determine if Nt5e presence correlates with CD73 protein, we performed co-immunofluorescence staining for CD73 and markers of hepatocytes, cholangiocytes, endothelial cells, and Kupffer cells (Figure 1E). In agreement with the

Most current article

Figure 1. CD73 is expressed primarily on hepatocytes in normal mouse liver. t-distributed stochastic neighbor embedding (tSNE) and violin plots showing RNA sequencing analysis of the mouse liver from (A and B) fluorescence-activated cell sorter (FACS)-sorted and (C and D) microfluidic droplet captured cells showing the highest expression of the mouse CD73-encoding gene *Nt5e* in hepatocytes. Data were obtained from Tabula Muris. (E) Fresh-frozen liver sections were stained with antibodies against CD73 (green), and the cell-specific markers keratins K8/18 (hepatocyte), K19 (cholangiocyte), CD31 (endothelium), and F4/80 (Kupffer cells) in red. *Bottom row*: Magnified views of the *boxed areas* in the *top row*. Blue, 4′,6-diamidino-2-phenylindole (DAPI)-stained nuclei (DNA). (F) Immunofluorescence staining for CD73 (green) in frozen liver sections showing co-localization with the bile-canalicular marker zonula occludens 1 (ZO1) (red). *Right*: 4× magnified view of the *boxed area* in the *merged panel*. DAPI-stained nuclei. Blue, DAPI-stained nuclei (DNA). *Scale bars*: 20 μm. NK, natural killer; LSEC, liver sinusoidal endothelial cell.
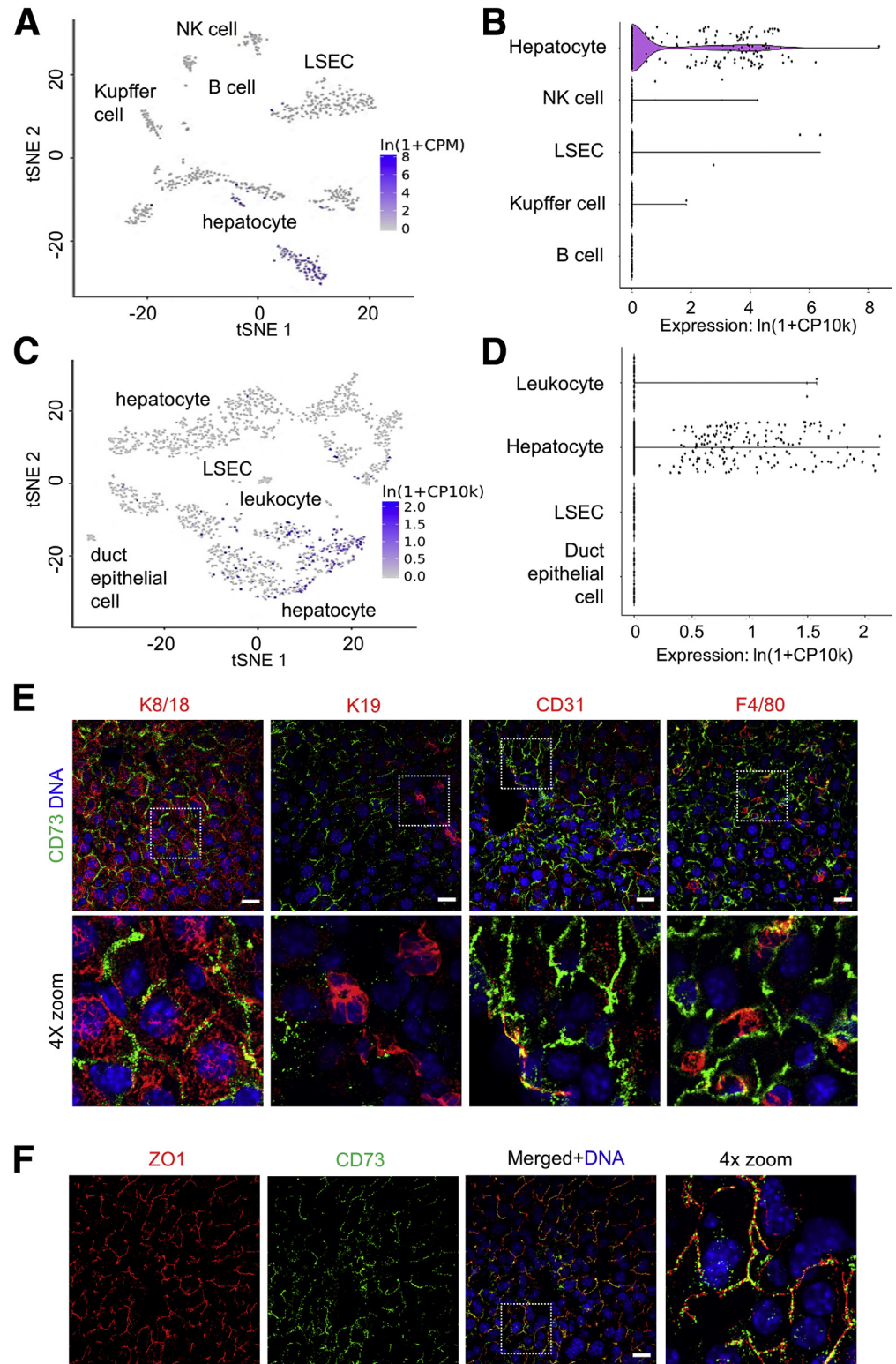
transcriptomic data, CD73 is present on hepatocytes, but absent from cholangiocytes, which are marked by keratin (K) K8/K18 and K19 staining, respectively (Figure 1E). In addition, subsets of endothelial cells, expressing CD31, and Kupffer cells, expressing F4/80, co-stained for CD73 (Figure 1E). However, the most abundant expression of CD73 was detected on the bile canalicular membranes of hepatocytes, as shown by co-staining with the tight junction marker protein zonula occludens 1 (Figure 1F).

Liver-Specific CD73 Knockout Mice Develop Normally and Do Not Show Major Liver Abnormalities at a Young Age

To address the function of CD73 in the mammalian liver, we generated mice with a targeted deletion of the *Nt5e* gene in hepatocytes. The critical exon 2 of *Nt5e* was flanked by loxP sites and deleted in the presence of Cre recombinase driven by the albumin (*Alb*) promoter. As expected, *Nt5e* was selectively targeted in the liver (Figure 2*A*) and CD73 protein was absent from primary hepatocytes isolated from the CD73-LKO mice (Figure 2*B*). Immunoblotting of total liver lysates showed that CD73 levels were reduced by 75% and 67% in male and female CD73-LKO mice, respectively, compared with age-matched wild-type (WT) mice (Figure 2*C* and *D*). The expression of a functionally related GPI-anchored protein, tissue nonspecific alkaline phosphatase, was unaffected (Figure 2*C*). Immunofluorescence analysis of liver tissues showed the absence of CD73 from the apical membrane of hepatocytes in CD73-LKO mice (Figure 2*E*), and this corresponded to significantly diminished *ecto*–adenosine monophosphatase (AMPase) activity in the pericentral region of CD73-LKO livers (Figure 2*F*). Therefore, the CD73-LKO mice lack hepatocyte CD73 expression and are deficient in CD73-associated ecto-AMPase function.

To determine how this genetic manipulation affected liver function, we analyzed mice at different ages. Histologic examination of liver tissues from 7-week-old WT and CD73-LKO male mice did not show major differences (Figure 3*A*). In agreement with previous observations using constitutive *Nt5e*-knockout mice,[22] the CD73-LKO mice did not show major defects in viability, growth, and development up to the mature adult stage at 21 weeks (Figure 3*B*). Both male and female CD73-LKO mice gained weight at the same rate (Figure 3*B*) and had similar liver weight–to–body weight ratios compared with their WT counterparts (Figure 3*C*). Taken together, these data show that hepatocyte CD73 is not required for normal mouse liver development and maturation.

CD73-LKO Mice Develop Spontaneous Hepatocyte Degeneration in a Sex- and Age-Dependent Manner

The zonal expression pattern of CD73 on pericentral hepatocytes prompted us to investigate the long-term consequences of CD73 deficiency because pericentral hepatocytes are important for the homeostatic renewal in the mouse liver.[29,30] Therefore, we studied the liver phenotypes of standard chow-fed WT and CD73-LKO mice between 22 and 42 weeks (5–10 mo) of age, which represents the period between the mature adult and middle-aged stages. Serum analysis showed a trend ($P < .08$) toward increased alanine aminotransferase levels in male mice, but not in female mice ($P < .3$) at 21–22 weeks of age (Figure 4*A*). Histologically, we observed significant pericentral hepatocyte injury in 22-week-old male CD73-LKO mice, which was not present in the female mice, or the corresponding age- and sex-matched WT controls (Figure 4*B*). The hepatocyte injury and tissue damage were more extensive in the older (age, 42 wk) compared with the younger (age, 22 wk) male mice (Figure 4*C*), pointing to a progressive and age-dependent liver injury. Blinded quantitative histologic analysis further unmasked male-predominant hepatocellular damage ($P < .05$), which was defined by swelling and ballooning hepatocyte degeneration (Figure 4*D*). Another notable sex difference was that hepatocytes in female CD73-LKO appeared smaller (Figure 4*B*), which corresponded with decreased serum albumin levels (Figure 4*E*), whereas serum albumin was unaffected in the male CD73-LKO mice (Figure 4*E*). Furthermore, we observed a significant increase in serum blood urea nitrogen levels in the male, but not female, CD73-LKO mice (Figure 4*F*).

Deficiency of Hepatocyte CD73 Leads to AMP-Activated Protein Kinase Hypoactivation and Perturbs Metabolic Homeostasis

To understand the cellular basis for the male-predominant histopathologic changes, we performed proteomic profiling on freshly isolated hepatocytes from 5-month-old male WT and CD73-LKO mice (Figure 5*A*). This analysis showed up-regulation in protein synthesis pathways associated with the transcriptional regulator eukaryotic initiation factor 2 (EIF2), apoptosis, and nucleotide excision repair. Pathways involved in fatty acid oxidation (peroxisome proliferator-activated receptor α/retinoid X receptor α, PPARα/RXRα), cholesterol, and stearate biosynthesis also were up-regulated (Figure 5*A*). On the other hand, hormone signaling (estrogen and aldosterone), amino acid metabolism (transfer RNA charging), nutrient sensing (mechanistic target of rapamycin, mTOR; p70S6K), and overall cellular energy homeostasis (oxidative phosphorylation and AMP-activated protein kinase [AMPK]) pathways were down-regulated in the CD73-null hepatocytes (Figure 5*A*). Consistent with abnormal lipid metabolism, as suggested by the proteomic analysis, male CD73-LKO mice developed significantly more microvesicular and macrovesicular steatosis, compared with female mice (Figure 5*B* and *C*). We profiled a set of lipid metabolism genes to determine if transcriptional compensation may account for the sex differences we observed. Although most genes remained unchanged, the gene *Hmgcs1*, which encodes hydroxymethylglutaryl-coenzyme A synthase, was significantly higher in female WT mice and further induced in the CD73-LKO mice (Figure 5*D*). Hydroxymethylglutaryl-CoA synthase converts acetyl-CoA to hydroxymethylglutaryl-CoA, which is used in the mevalonate pathway.

To further examine the link between CD73 activity and hepatic lipid accumulation, we treated WT hepatocytes
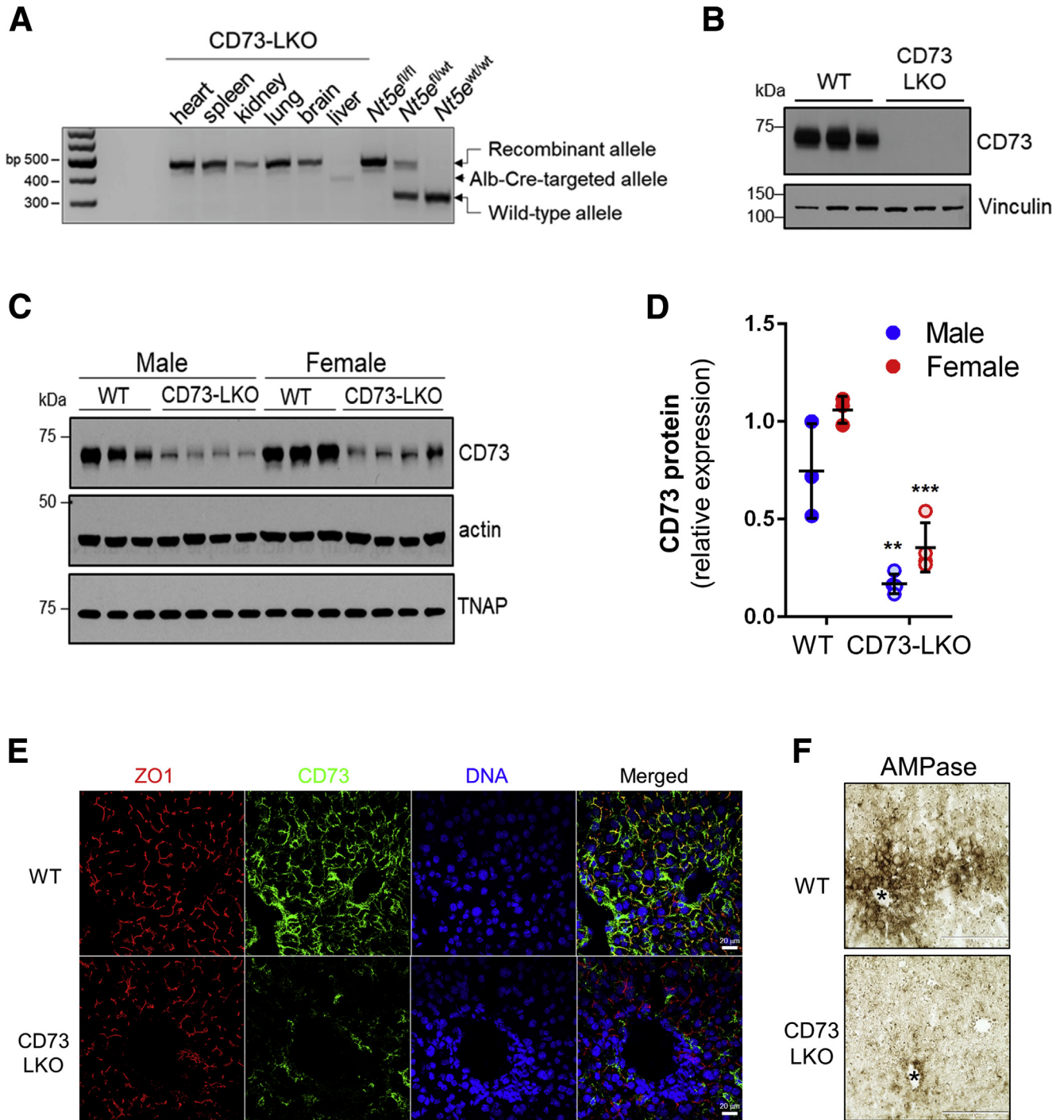
Figure 2. Generation of liver-specific CD73-LKO mice. (*A*) PCR analysis of *Nt5e* generated a 349-bp fragment from the Cre-targeted allele in the CD73-LKO mouse liver. *Nt5e*(wt/wt), *Nt5e*(fl/wt), and *Nt5e*(fl/fl) mice are controls. Representative immunoblots of CD73 in (*B*) primary hepatocytes, and (*C*) in total liver lysates from male and female WT and CD73-LKO mice. Actin and tissue nonspecific alkaline phosphatase (TNAP) immunoblots serve as controls. (*D*) Semiquantitative analysis of CD73 protein expression based on immunoblot band intensities in panel *C*. **$P < .01$, ***$P < .001$, 2-way analysis of variance. Error bars represent SD. (*E*) Immunofluorescence staining for CD73 (green), tight junction protein zonula occludens 1 (ZO1) (red), and 4′,6-diamidino-2-phenylindole (DAPI)-stained DNA (blue) on frozen liver tissue sections from WT (*top*) and CD73-LKO (*bottom*) mice. *Scale bar*: 20 μm. (*F*) AMPase activity in WT and CD73-LKO mice using formalin-fixed liver tissue sections. The brown deposits indicate ecto-AMPase activity in the presence of AMP. *Stars* indicate the central vein. *Scale bar*: 400 μm.
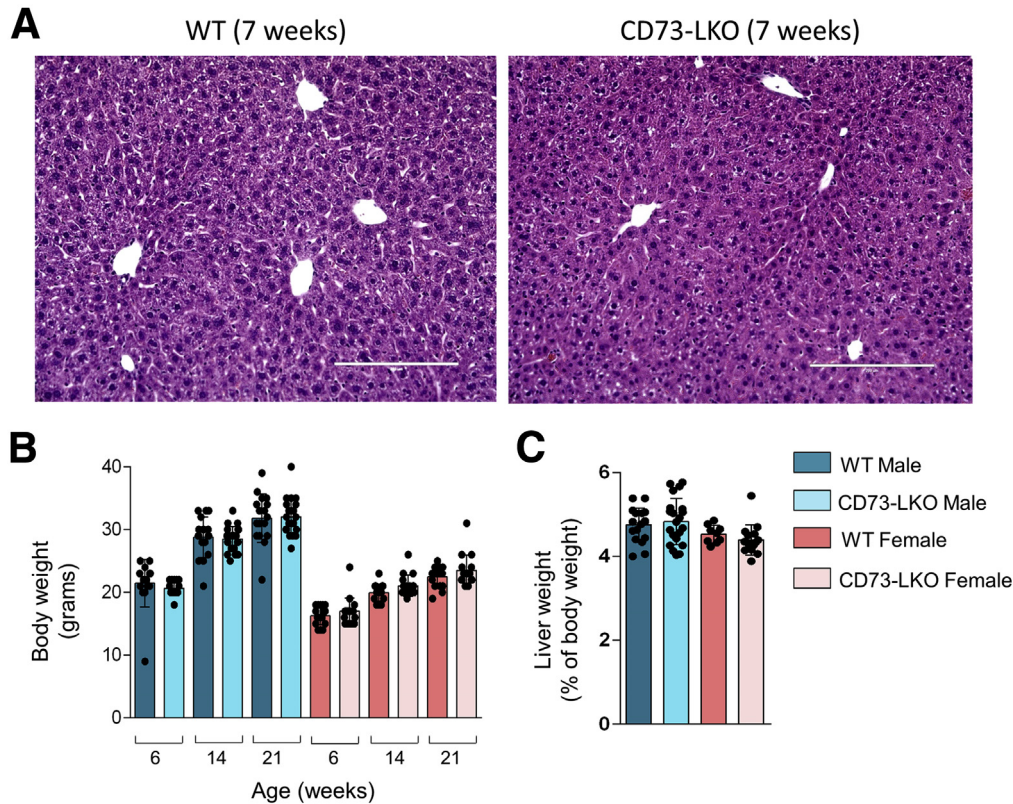
Figure 3. CD73-LKO mice develop normally and do not show major liver abnormalities up to 21 weeks of age. (*A*) Formalin-fixed liver sections of 7-week-old male mice stained with H&E. *Scale bar*: 200 μm. (*B*) Comparison of body weight from WT and CD73-LKO mice at 6–21 weeks of age. n = 15–21 mice/group. (*C*) Analysis of liver-to-body weight ratios of 21-week-old mice. Males: n = 18 WT, n = 21 CD73-LKO. Females: n = 9 WT, n = 15 CD73-LKO. Error bars represent SD.

with the CD73 inhibitor adenosine 5'-(α,β-methylene) diphosphate (APCP) in the absence and presence of oleic acid and monitored neutral lipid accumulation using a fluorescence imaging method. Treatment with APCP alone led to significant accumulation of lipid droplets in hepatocytes (Figure 6*A* and *B*). Co-treatment of hepatocytes with oleic acid and APCP together led to significantly more accumulation of lipid droplets than either treatment alone (Figure 6*A*), suggesting that CD73 enzymatic activity regulates hepatocyte lipid metabolism. To determine if CD73 enzymatic activity is altered during hepatic steatosis, we fed mice a high-fat diet (HFD) for 14 weeks and assessed CD73 ecto-AMPase activity using enzyme histochemistry. As shown in Figure 6*C*, hepatic steatosis leads to a dramatic decrease in CD73 activity in vivo. Together with the results in isolated hepatocytes, this suggests that CD73 enzymatic activity and hepatic lipid metabolism are closely linked.

The proteomic profiling showed that AMPK, which is an ATP sensor and master metabolic regulator of lipid and glucose homeostasis, was down-regulated in CD73-LKO hepatocytes. To determine if the metabolic dysregulation in the absence of CD73 was linked to altered AMPK signaling, we probed for AMPK substrate phosphorylation using a specific phospho-motif antibody targeting LXRXX [pS/pT].[31] Despite equal expression of total AMPKα, male CD73-LKO mice had a dramatic reduction in the phosphorylation of AMPK substrates (Figure 7*A* and *B*). On the other hand, baseline AMPK substrate phosphorylation was lower in WT female mice and

was not changed significantly by CD73 deletion. The down-regulation of AMPK substrate phosphorylation was not related to major changes in the abundance or subcellular distribution of the kinase (Figure 7*C*), leading us to hypothesize that adenosine generated by CD73 promotes AMPK activity. In support of this hypothesis, extracellular addition of AMP significantly, and dose-dependently, induced AMPK activation (phosphorylation at Thr-172) in primary hepatocytes co-treated with soluble, enzymatically active CD73 (Figure 7*D* and *E*). To determine if this effect was dependent on the uptake of extracellular adenosine, we tested AMPK activation in the absence and presence of nitro-benzylthioinosine, an inhibitor of the equilibrative nucleoside transporter 1 adenosine re-uptake transporter.[32] Although AMPK phosphorylation appeared blunted in the presence of nitrobenzylthioinosine, this was not statistically significant (Figure 7*F*–*G*), suggesting multiple potential mechanisms. Combined, these data show that CD73, in the presence of extracellular AMP, activates AMPK in hepatocytes potentially via transport-dependent and independent mechanisms.

Mature Adult CD73-LKO Mice Develop Liver Inflammation, With a Male Predominance in Severity

Because CD73 and adenosine play a major role in immune suppression, we next asked whether CD73-LKO mice develop hepatic inflammation. Blinded histologic analysis showed the presence of portal and lobular inflammation
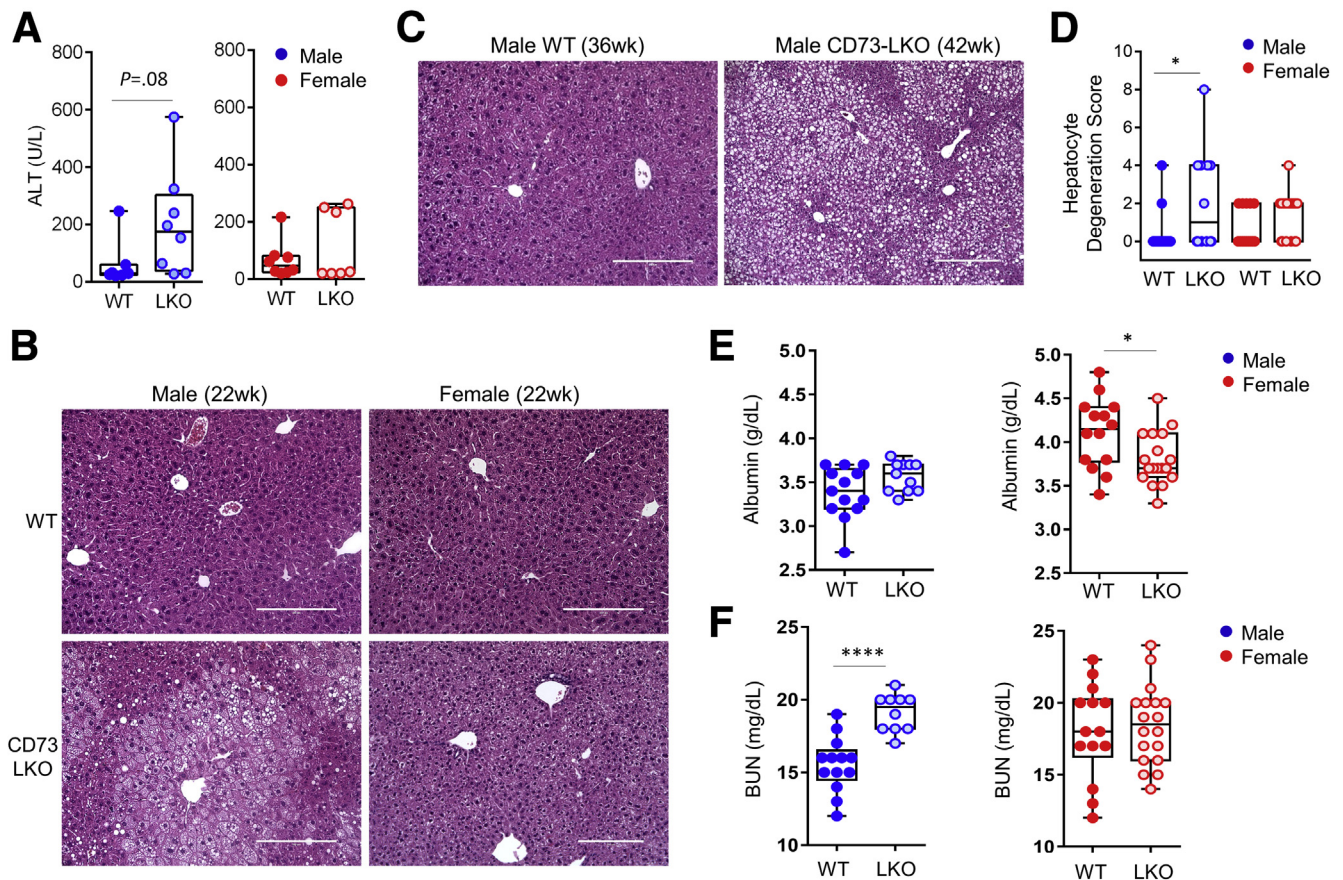
Figure 4. CD73-LKO mice develop spontaneous liver injury after 21 weeks of age in a sex-dependent manner. (*A*) Serum analysis of alanine aminotransferase (ALT) in 21- to 22-week-old male (blue) and female (red) WT (*filled circles*) and CD73-LKO mice (*open circles*). Males: n = 8 WT; n = 8 CD73-LKO; *P* = .08 (unpaired *t* test); females: n = 7 WT; n = 7 CD73-LKO. *P* = .3 (unpaired *t* test). (*B*) Representative H&E images of formalin-fixed liver sections from 22-week-old male and female WT and CD73-LKO mice. *Scale bars*: 200 μm. (*C*) Representative H&E images of formalin-fixed liver sections from 36- to 42-week-old male WT and CD73-LKO mice. *Scale bars*: 200 μm. (*D*) Quantification of blinded histologic scoring of hepatocyte degeneration (defined as swelling and ballooning) in 21- to 42-week-old mice. Scoring: 0, none; 4, mild swelling/focal ballooning; 8, severe swelling/extensive ballooning (scores were averaged for animals with ballooning + swelling). *$P < .05$; 1-way analysis of variance. Box-and-whisker plots of (*E*) albumin and (*F*) blood urea nitrogen (BUN) in male (blue) and female (red) WT (*filled circles*) and CD73-LKO mice (*open circles*). Same animals as in panel *D*. Males: n = 13 WT; n = 12 CD73-LKO; females: n = 14 WT; n = 18 CD73-LKO mice. *$P < .05$, ****$P < .0001$; unpaired *t* test.

in both male and female CD73-LKO mice, but the male mice were affected more severely (Figure 8*A* and *B*). Consistent with the known roles of adenosine[33] and AMPK[34] as anti-inflammatory mediators, we observed induction in the proinflammatory cytokines interleukin 1β and tumor necrosis factor α in the CD73-LKO livers, with the latter reaching statistical significance only in female mice (Figure 8*C*). Despite the similar transcriptional changes of proinflammatory genes, male mice showed significantly more neutrophil infiltration, as assessed by lymphocyte antigen 6 complex locus G6D (Ly6G) staining (Figure 8*D* and *E*). Profiling of CD73-associated adenosine pathway components, including the AMP substrate-generating enzyme CD39 (*Entpd1*) and adenosine receptors A1, A2A, A2B, and A3 (*Adora 1, 2A, 2B,* and *3*), showed female-specific compensatory induction of these targets in the absence of hepatocyte CD73 (Figure 8*F*). These results show that loss of hepatocyte

CD73 leads to spontaneous liver inflammation, and that in female mice this may be partly opposed by compensatory up-regulation of anti-inflammatory adenosine signaling mediators to limit tissue damage.

Discussion

Physiological Hepatoprotection of CD73 and Adenosine

Our study shows the importance of CD73, a major extracellular AMPase, for the long-term metabolic integrity of the mammalian liver. Previous seminal work using constitutive CD73 knockout mice established CD73 as a key factor in maintaining epithelial integrity via adenosine-mediated protection of the tissue barrier function, especially during hypoxia,[19,22,35,36] while our present findings provide new insights into the homeostatic mechanisms that are attributed specifically to CD73 on hepatocytes.
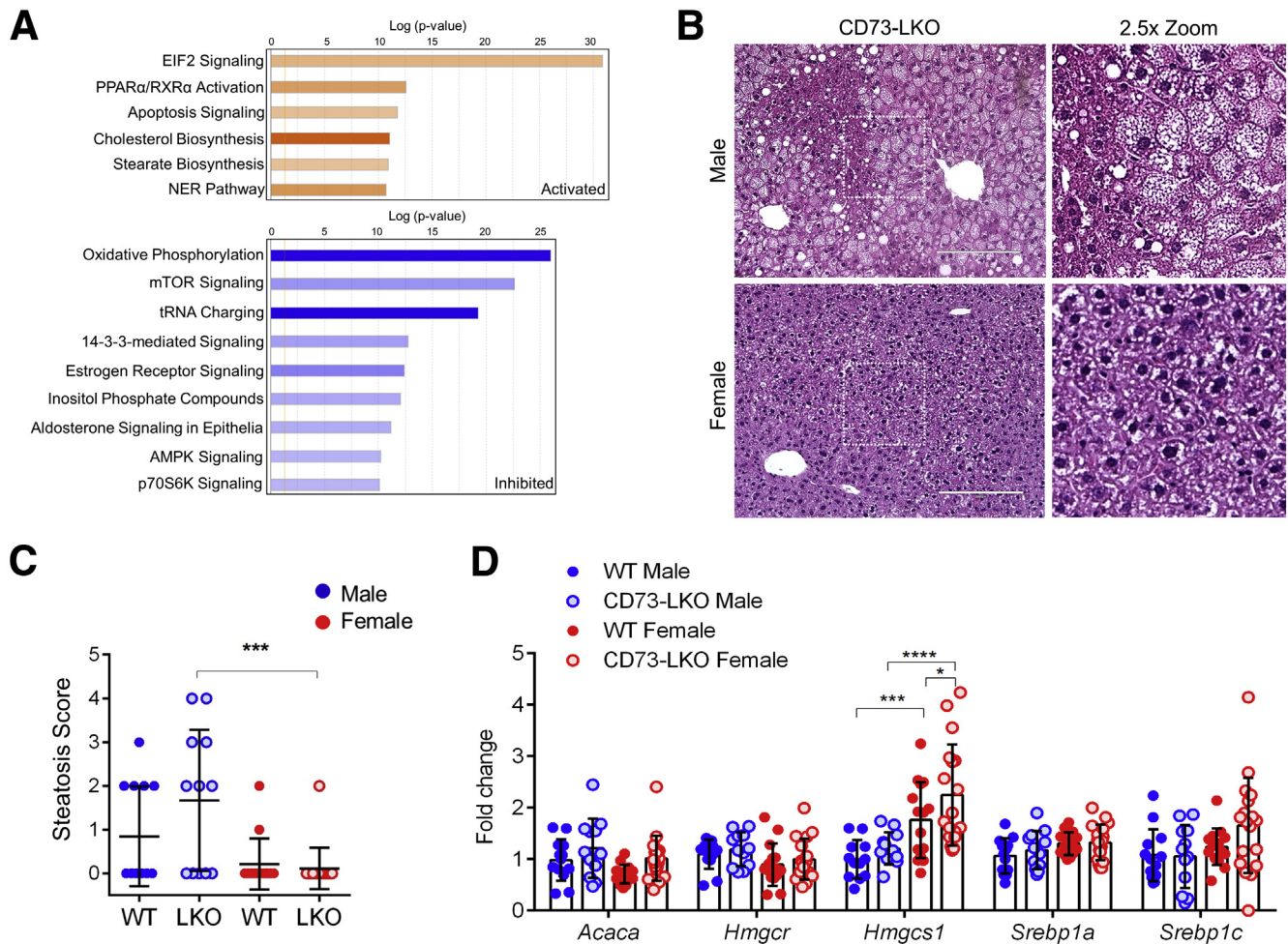
Figure 5. Metabolic imbalance and increased steatosis in male CD73-LKO mouse hepatocytes and livers. (*A*) Ingenuity pathway analysis of proteomic results showing activated (*orange*) and inhibited (*blue*) pathways in freshly isolated hepatocytes from male CD73-LKO mice relative to WT controls. (*B*) H&E staining of formalin-fixed liver sections. Magnified view of *boxed areas* in the *left panel* comparing the presence of steatosis in male and female CD73-LKO mice. *Scale bar*: 200 μm. (*C*) Quantification of blinded histologic scoring of microvesicular and macrovesicular steatosis. Scoring: 0, none; 1, mild; 2, moderate; 3, severe (scores were averaged for animals with microsteatosis and macrosteatosis). Males: n = 13 WT; n = 12 CD73-LKO; females: n = 14 WT; n = 18 CD73-LKO. ***$P < .001$, 1-way analysis of variance. (*D*) Gene expression analysis of lipid metabolism genes *Acaca*, *Hmgcr*, *Hmgcs1*, *Srebp1a*, and *Srebp1c* using total liver messenger RNA in male and female WT and CD73-LKO mice. n = 13 WT male, n = 12 LKO male, n = 14 WT female, n = 18 LKO female. *$P < .05$, ***$P < .001$, ****$P < .0001$, 2-way analysis of variance. Error bars represent SD. EIF2, eukaryotic initiation factor 2; NER, nucleotide excision repair; PPARα/RXRα, peroxisome proliferator-activated receptor α/retinoid X receptor α; tRNA, transfer RNA.

The male-predominant, spontaneous development of liver disease that we observed in CD73-LKO mice points to a physiological protective mechanism of CD73 that shows a sexual dimorphism. We conclude that AMPK hypoactivation, likely secondary to extracellular adenosine deficiency, contributes to hepatocellular injury, metabolic stress, and inflammation in male CD73-LKO mice. CD73 is down-regulated significantly under conditions of severe and persistent chronic stress in the mouse liver,[13] and in chronic human liver diseases of different etiologies.[14,15] Future studies addressing the detailed mechanisms of how CD73 supports metabolic homeostasis in hepatocytes throughout the lifespan, and in a sex-dependent manner, will have important implications for understanding mammalian liver biology as well as disease

development and progression. To that end, the *Nt5e*^{fl/fl} and CD73-LKO mice represent tools for studying the cell-specific mechanisms of human liver diseases that are driven by perturbed metabolism and inflammation, such as NAFLD.[37]

Sex Differences and Hormonal Regulation of the CD73-Adenosine Axis Across the Lifespan

At present, we do not fully understand the genetic and metabolic factors contributing to the sex differences. Our findings here highlight the importance for future work to consider both biological sex and age when examining the role of CD73-adenosine in hepatocyte biology and liver disease. Previous reports using whole-body knockout mice to address
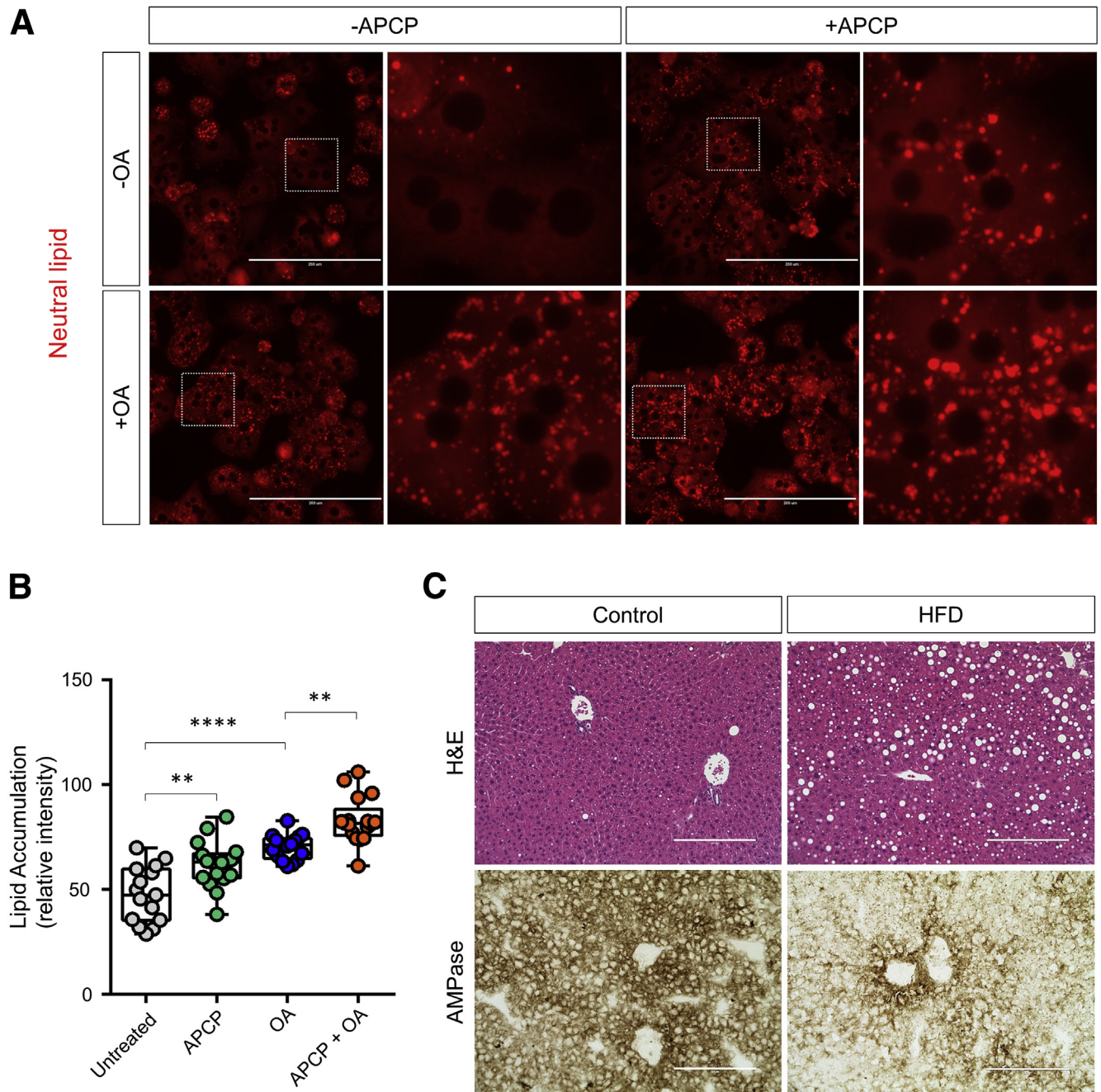
Figure 6. Inhibition of CD73 enzymatic activity promotes lipid accumulation in hepatocytes. (*A*) Isolated WT C57BL/6 male hepatocytes were treated for 24 hours with 1 μmol/L oleic acid in the presence or absence of the CD73 inhibitor, APCP (10 μmol/L). Intracellular lipid accumulation was analyzed using LipidTOX neutral lipid stain (*red*). (*B*) Quantification of lipid accumulation in panel *A*. **$P < .01$, ****$P < .0001$; 1-way analysis of variance. Error bars represent SD. (*C*) WT mice were fed normal chow (Control) or a HFD for 14 weeks. *Top panels*: Representative H&E images of Control- and HFD-fed mice, showing the development of steatosis in the HFD condition. *Bottom panels*: Representative enzyme histochemistry images showing a decrease in CD73 AMPase activity in the HFD condition. *Scale bars*: 200 μm.

the role of CD73 and adenosine in hepatic steatosis[38] and fibrosis[39] examined only young (age, 6–8 wk) male mice. We found that 7-week-old CD73-LKO mice are indistinguishable from their WT littermates, regardless of sex, whereas CD73 loss is detrimental at older ages, but that female mice are relatively protected. Our study shows sex-dependent liver injury resulting from CD73 deficiency, and the CD73-

adenosine axis has been linked recently to the protective action of female sex hormones in other organ systems and diseases. For example, estrogen-receptor signaling maintains CD73 expression and adenosine production by osteoprogenitors, while the loss of CD73-generated adenosine promotes postmenopausal bone loss in mice.[40] In addition, several studies have shown complex and region-specific modulation
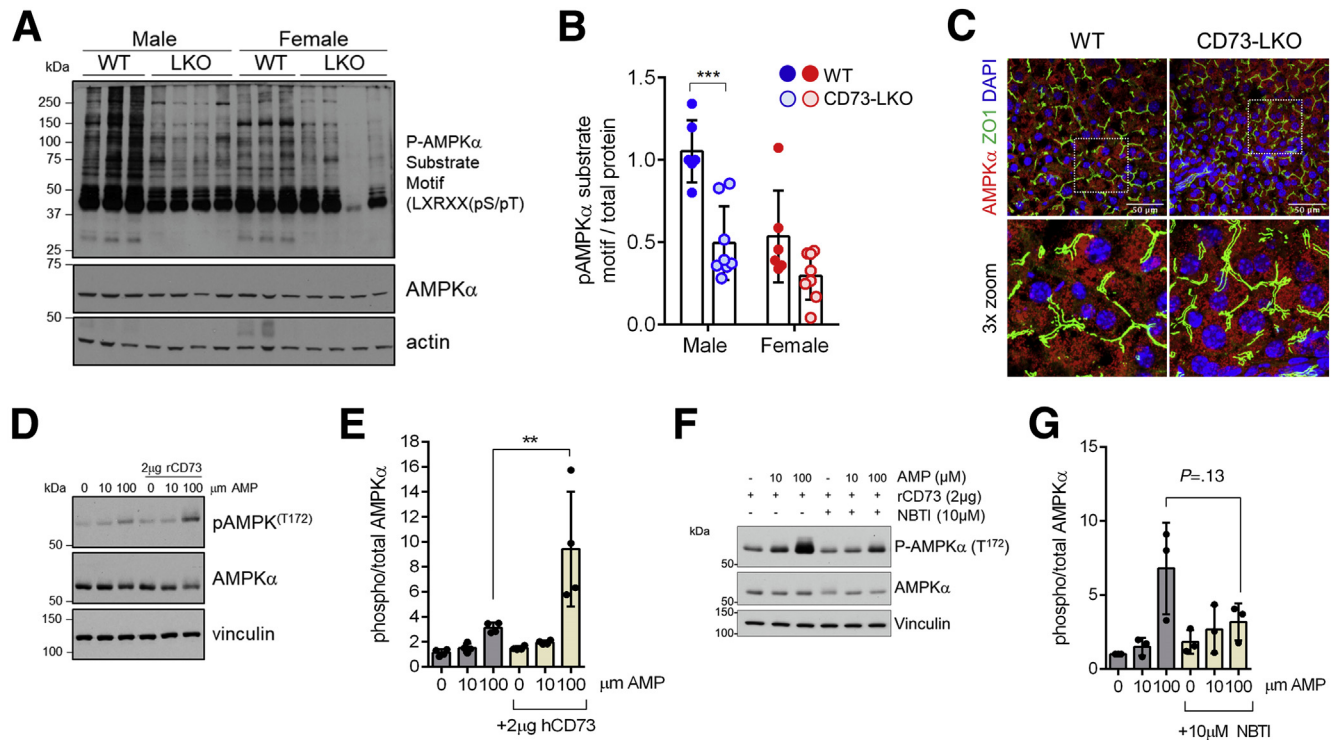
Figure 7. CD73-generated extracellular adenosine activates AMPK in hepatocytes and livers from CD73-LKO mice and show impaired AMPK signaling. (*A*) Representative immunoblots of AMPK substrate phosphorylation in liver lysates from male and female mice. (*B*) Semiquantitative analysis of AMPK substrate phosphorylation relative to total protein based on immunoblots in panel *A*. ***P < .0001, 2-way analysis of variance. Error bars represent SD. (*C*) Fresh-frozen liver sections were stained with antibodies against AMPK (*red*) and zonula occludens 1 (ZO1) (*green*) show similar AMPK distribution in WT and CD73-LKO mice. *Bottom panels*: Magnified view of the *boxed areas*. *Scale bar*: 50 μm. (*D*) Isolated WT hepatocytes were treated with AMP and recombinant soluble CD73 (rCD73) at the indicated concentrations. Representative immunoblots of total and phospho-AMPKα. (*E*) Quantification of phosphorylated/total AMPK. n = 4 replicates. **P < .001; 2-way analysis of variance. (*F*) Representative immunoblot analysis showing AMPK phosphorylation in WT hepatocytes treated with AMP, rCD73, and the adenosine transport inhibitor nitrobenzylthioinosine (NBTI). (*G*) Quantification of phosphorylated/total AMPK in rCD73-treated hepatocytes, in the absence/presence of AMP and NBTI. n = 3 replicates. 2-way analysis of variance. Error bars represent SD. DAPI, 4′,6-diamidino-2-phenylindole.

of spontaneous adenosine production by CD73 in the central nervous system that is mediated by both estrogen receptors α and β,[41–43] accounting for sex differences underlying adenosine-dependent neuromodulation. Although the exact significance of increased Hmgcs1 in the female mice is not presently clear, it is possible that it serves a protective mechanism against lipid accumulation because deficiency of the closely related mitochondrial Hmgcs2 gene promotes mouse fatty liver pathology via ketogenic insufficiency.[44] Moreover, it was shown recently that, in regulatory T cells, perturbation of the mevalonate pathway leads to metabolic stress and a dramatic reduction in cell surface CD73 expression,[45] showing a link between these 2 pathways.

Biological sex and reproductive hormones exert a significant effect over individual variability to human disease development and progression.[46] This is especially evident in chronic liver disease, which currently ranks among the top 10 causes of death in men, but not in women.[47] Both male sex and older age are associated with worse survival and greater incidence of HCC among patients with biopsy-confirmed NAFLD.[48] However, the basic biological mechanisms of how age and biological sex affect patient susceptibility to disease development and progression have

been difficult to understand, especially in the case of NAFLD.[49] Recent studies in mice have shown that the genetic background, body fat distribution, plasma high-density lipoprotein, ceramide, and metabolic gene (eg, *Pklr*, *Lcn2*) levels underlie sex differences in hepatic steatosis.[50–54] An extensive analysis examined 50 metabolic and cardiovascular traits in 100 inbred mouse strains and showed significant sex differences at the molecular and physiological levels.[54] In general, sex hormones partially accounted for the metabolic traits, but the major conclusion from this study was that sex differences cannot be reconciled by examining single molecules or even pathways, given the multitude of variables that exert effects on the organism (eg, environment, age, genetic background) and their interactions. Therefore, the CD73-adenosine axis is one of many pathways that can influence sex differences in liver biology and disease.

Cross-Talk Between CD73 and AMPK in Hepatocytes

CD73 is strongly induced in epithelial tissues under hypoxic conditions via hypoxia-inducible factor-1.[19] Rapid and sustained CD73 up-regulation during hepatic ischemia
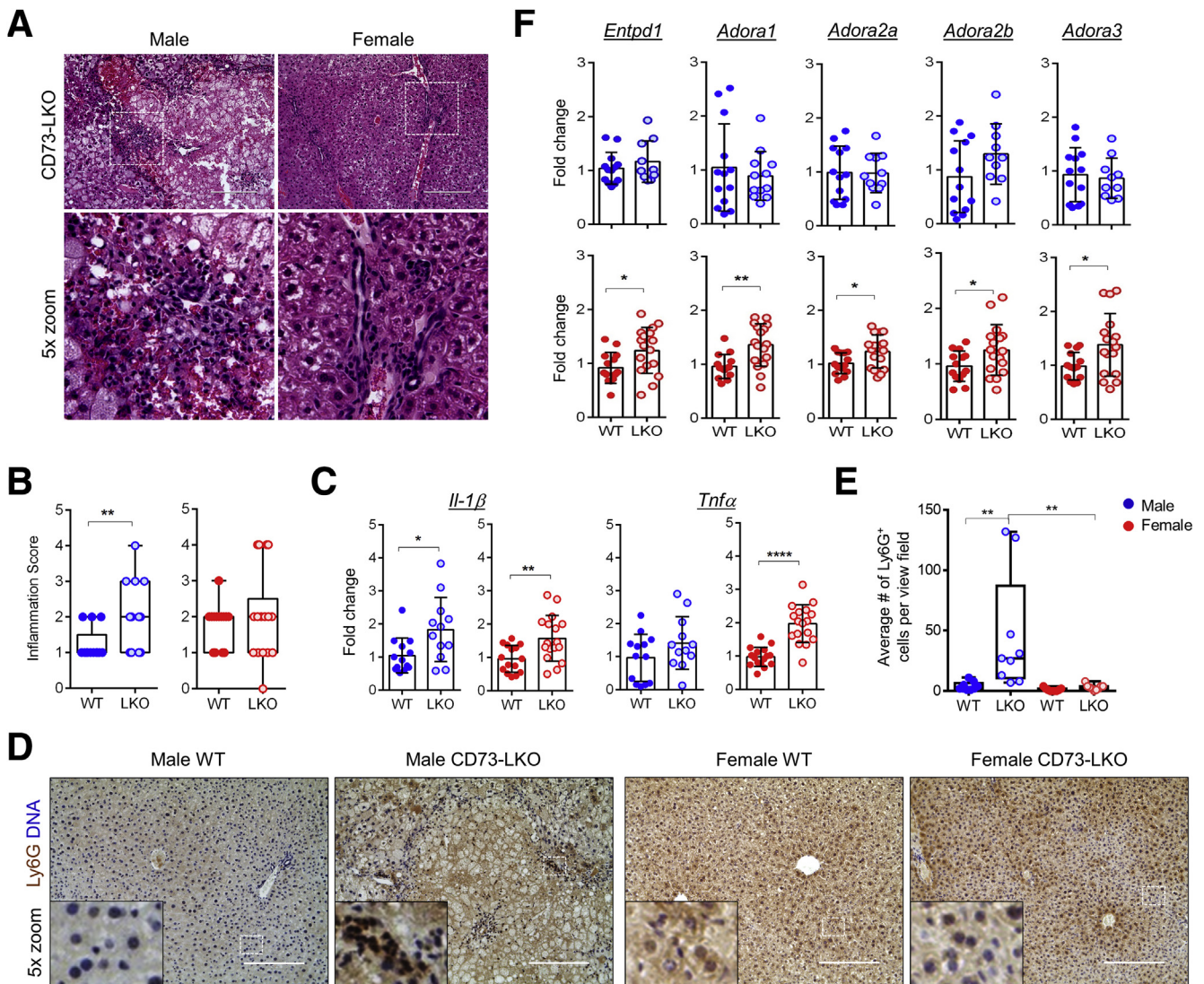
Figure 8. Loss of hepatocyte CD73 results in spontaneous liver inflammation. (*A*) Representative H&E images of inflammatory lesions in livers from 22-week-old CD73-LKO mice. *Boxed areas* in the *top panels* are magnified in the *bottom panels*. (*B*) Quantification of blinded histologic analysis of portal and lobular inflammation (scores were averaged for animals with portal + lobular inflammation). Scoring: 0, none; 2, minimal; 4, mild; 6, moderate; 8, severe. (*C*) Total liver messenger RNA analysis of proinflammatory markers interleukin 1β and tumor necrosis factor α in male (blue) and female (*red*) mice aged 21–42 weeks. (*D*) Representative images of immunohistochemical-stained paraffin-embedded liver tissues for neutrophil marker Ly6G (*brown*). Harris hematoxylin-stained nuclei (blue). *Inset*: magnified view of the *boxed area* showing signal distribution. *Scale bar*: 200 μm. (*E*) Quantification of Ly6G$^+$ cells per view field in panel *D*. (*F*) Gene expression analysis of ectonucleotidase CD39 (*Entpd1*) and adenosine receptors A1R, 2AR, 2BR, and 3R (*Adora1, 2a, 2b, 3*) using total liver messenger RNA in male and female WT and LKO mice. n = 13 WT male, n = 12 LKO male, n = 14 WT female, n = 18 LKO female. *P < .05, **P < .01, ****P < .0001, unpaired t test. Error bars represent SD.

confers adenosine-dependent hepatoprotection.[21] The latter is very similar to the reported hepatoprotective effect of AMPK during ischemic preconditioning,[55] although a functional link between these pathways has not been established. At 5 months of age, AMPK activity in mouse liver is augmented significantly by hypoxia, but this regulation is lost at older ages.[56] The age-dependent activation of AMPK by hypoxia in the liver coincides with the age of onset of spontaneous liver injury in the CD73-LKO

mice, which became apparent at 5 months in our study. Based on this, we propose that the detrimental effects stemming from CD73 deficiency in hepatocytes may be associated with impaired capacity of the mature liver to calibrate oxygen responses properly via AMPK. In vitro work in cell lines, and in vivo studies using lower organisms, have linked AMPK and hypoxia-inducible factor-1 cross-talk with cellular homeostasis and organismal longevity through their roles in

balancing intracellular reactive oxygen species.[57,58] The purinergic signaling pathway also plays important roles in oxidative stress responses in the liver and is disrupted in liver disease.[59] As a key regulator of purinergic signaling, and the major extracellular enzymatic source of the immunosuppressive and anti-inflammatory mediator adenosine, CD73 represents a promising target for metabolic inflammation, which is considered a major driver of chronic human diseases and associated comorbidities.[39,60]

Anti-inflammatory Effects of Adenosine in the Liver

In various liver injury models, adenosine exerts protective anti-inflammatory effects through the activation of the G_s-protein–coupled adenosine receptor 2A ($A_{2A}R$) on hepatocytes and immune cells.[35,61,62] For example, genetic deletion or pharmacologic inhibition of the $A_{2A}R$ causes severe inflammation and liver damage after concanavalin A–induced liver injury in a mixed cohort of male and female mice.[61] Whole-body hypoxia treatment provided protection against concanavalin A–induced liver inflammation.[62] Although the detailed mechanism behind the hepatoprotective effects of hypoxia in liver inflammation are not clear, it is plausible that hypoxia-mediated CD73 induction, followed by increased extracellular adenosine production, may be important during immune-mediated liver damage, which remains to be examined in detail in future studies. CD73 protein was shown to be up-regulated in a HFD model of liver injury performed in male mice, in which the hepatic protein expression of CD39 and $A_{2A}R$ also were increased.[35] The up-regulation of these purinergic factors was likely a protective mechanism because the absence of $A_{2A}R$ led to more severe inflammation, steatosis, and impaired insulin sensitivity after HFD feeding.[35]

The hypoactivation of AMPK and liver injury in the CD73-LKO mice that we observed were similar to the findings from another study using a mixed cohort of older (age, 12–16 mo) male and female mice, which found that the absence of the $A_{2A}R$ receptor leads to hypoactivation of AMPK and metabolic dysregulation, specifically obesity, hyperglycemia, and glucose intolerance.[63] The relative protection that we observed in the female CD73-LKO mice in our study could be attributed to compensatory induction of adenosine receptors, in particular $A_{2A}R$ and $A_{2B}R$. Paradoxically, our proteomic analysis showed that the mTOR pathway is decreased in CD73-LKO mice despite the AMPK hypoactivation. It is plausible that the decrease in mTOR activity as predicted by the proteomic analysis is secondary to nucleotide imbalance because it recently was shown that mTOR is inhibited by purine depletion (adenylate and its derivatives) irrespective of AMPK activation.[64] Specifically, genetic and pharmacologic blockade of de novo purine biosynthesis or purine salvage significantly decreased the activation of the key mTOR downstream targets S6K and 4EBP1. This inhibitory effect was rescued by exogenous purines and their intracellular conversion to adenylate nucleotides.

Taken together, our study provides broad insight into potential novel and sex-dependent functions of CD73 in promoting hepatocyte metabolic homeostasis under physiological conditions. Future studies will illuminate deeper understanding of the mechanistic networks by which CD73 plays a role in the liver. Ultimately, our findings can improve target identification for drug discovery in chronic liver diseases.

Materials and Methods
Chemicals and Reagents

The following chemicals and reagents were purchased from Sigma-Aldrich (St. Louis, MO): bovine serum albumin (A2153), adenosine 5′-(α,β-methylene)diphosphate (M3763), insulin (I0516), glucagon (G2044), hydrocortisone (H0888), levamisole (196142), calcium chloride dihydrate (223506), glucose (G8270), Percoll (P1644), and ethylene glycol-bis(β-aminoethyl ether)-N,N,N′,N′-tetraacetic acid (E3889). Laemmli sample buffer (4×, 1610747) was purchased from Bio-Rad Laboratories (Hercules, CA).

Generation of Hepatocyte-Specific CD73 KO Mice

CD73 floxed (CD73$^{fl/fl}$) mice were generated by Cyagen Bioscience, Inc (Santa Clara, CA). Briefly, exon 2 of the CD73-encoding gene, Nt5e (GenBank accession number: NM_011851.4; Ensembl: ENSMUSG00000032420), was targeted to generate a frameshift mutation from downstream exons. Bacterial artificial chromosome (BAC) clone RP23-137M4 from the C57BL/6J library was the template for the targeting vector that contains a Neo cassette flanked by Frt sites, and Nt5e exon 2 region flanked by loxP sites. Linearized targeting vector was electroporated into embryonic stem cells, followed by neomycin selection of resistant clones. Targeted embryonic stem clones were injected into blastocysts and transferred into surrogate mothers to obtain chimera lines. The conditional knockout allele was obtained after flippase-mediated recombination. Heterozygote (flox/wt) mice were bred with each other to obtain flox/flox. For this study, CD73$^{fl/fl}$ mice were backcrossed to C57BL/6J WT mice 4 times. To generate the CD73 hepatocyte-specific knockout mice (CD73-LKO), CD73$^{fl/fl}$ mice were bred with Cre mice driven by the albumin promoter (stock 003574; The Jackson Laboratory).[65] Genotyping was performed at 7–10 days of age and the mice were weaned at 21 days. WT and CD73-LKO littermates were maintained on a normal chow diet or a 14-week high-fat diet (60% calories from fat [Bio-Serv, Flemington, NJ]; as noted in Figure 6 legend) in the pathogen-free animal facility at the University of North Carolina at Chapel Hill. All experiments were approved by the Institutional Animal Care and Use Committee and in accordance with the National Institutes of Health guidelines.

Genotyping

Polymerase chain reaction (PCR) analysis using DNA extracted from toe clips and DreamTaq Green PCR Master

Mix 2× (K1081; Thermo Fisher, Waltham, MA) was performed to identify WT and CD73-LKO mice. Floxed PCR analysis used primers Floxed–Forward (5'-AGCACATTTAGTTTGAAATCCC-3'), and Floxed–Reverse (5'-AAACAGACTTCTTGATTGGCAT-3'). To identify the presence of Cre recombinase, we used primers Fabpi-200R (5'-TAGAGCTTTGCCACATCACAGGTCATTCAG-3'), Fabpi-200F (5'-TGGACAGGACTGGACCTCTGCTTTCCTAGA-3'), Cre-281R (5'-TCGCCATCTTCCAGCAGG-3'), and Cre-281F (5'-CCATCTGCCACCAGCCAG-3'). Amplicons were analyzed using 2% agarose gel electrophoresis. The presence of a 426-bp and 286-bp bands indicate a floxed CD73 and WT allele, respectively. A 300-bp and 200-bp band is positive for Cre recombinase.

Serum Analysis

Blood was collected by cardiac puncture from male and female WT and CD73-LKO mice between 5 and 9 months of age. Serum was analyzed for alanine aminotransferase, albumin, and blood urea nitrogen levels using the VetScan VS2 Analyzer and VetScan mammalian liver profile reagent rotor (Abaxis, Union City, CA).

Immunoblot

Total liver protein lysates were extracted from 25 mg of liver tissue from the left lobe or from cultured primary WT hepatocytes using ice-cold lysis buffer (50 mmol/L n-octyl-β-D-glucopyranoside, 1× protease inhibitors [05892970001; Roche, Basel, Switzerland], and 1× phosphatase inhibitors [04906837001; Roche] in 1× phosphate-buffered saline [PBS]). Protein lysates were resolved in 10% sodium dodecyl sulfate–polyacrylamide electrophoresis gels and transferred to a nitrocellulose membrane. After blocking in 5% milk in Tris-buffered saline with 0.1% Tween20 (TBST) for 1 hour at room temperature, the membranes were incubated with anti-CD73 (clone D7F9A, 13160), phospho-AMPKα (T172, clone 40H9, 2535), total AMPKα (clone D5A2, 5831), phospho-AMPK substrate motif (LXRXX [pS/pT], 5759S; Cell Signaling, Beverly, MA); pan actin (ACTN05, MA5-11869; Thermo Fisher), and antivinculin (clone hVIN-1, V9131; Sigma-Aldrich, St. Louis, MO) in 5% bovine serum albumin/TBST overnight at 4°C. Secondary antibodies (A4416, A6154, 1:5000–10,000; Sigma-Aldrich) were incubated for 1 hour at room temperature in 5% milk/TBST. Gels were stained with Coomassie blue, and membranes were stained with Ponceau S stain.

Primary Hepatocyte Isolation and Treatment

Hepatocyte isolation was performed on 5-month-old CD73$^{fl/fl}$ mice weighing 20–35 g. Mice were anesthetized with Avertin (250–300 mg/kg, intraperitoneally) (T48402; Sigma-Aldrich) to achieve deep anesthesia. The portal vein was cannulated and the liver was perfused with 50 mL of 37°C sterile buffer I solution (0.50 mmol/L ethylene glycol-bis[β-aminoethyl ether]-N,N,N',N'-tetraacetic acid, 5.5 mmol/L glucose, 1% penicillin/streptomycin in calcium- and magnesium-free Hank's balanced salt solution) at a rate

of 7 mL/min. Liver digestion was performed with 40 mL of 37°C sterile buffer II solution (1.5 mmol/L CaCl$_2$, 5.5 mmol/L glucose, 1% penicillin/streptomycin, and 3600 U of collagenase IV in calcium- and magnesium-free Hank's balanced salt solution) at a rate of 7 mL/min. Livers were surgically removed and hepatocytes were isolated in cold 1× Dulbecco's modified Eagle medium/penicillin/streptomycin media by size exclusion using 100-μm and 70-μm filters, respectively. Isolated hepatocytes were treated 24 hours after isolation with soluble human recombinant CD73 protein, AMP substrate, and a selective equilibrative nucleoside transporter 1 inhibitor, as specified in the figure legends. For intracellular lipid accumulation experiments, isolated WT C57BL/6 male hepatocytes were treated for 24 hours with 1 μmol/L oleic acid in the presence or absence of the CD73 inhibitor, APCP (10 μmol/L). Lipid accumulation was visualized using LipidTOX neutral lipid stain (H34477; Thermo Fisher). Fluorescence intensities were quantified in individual hepatocytes using Adobe Photoshop (San Jose, CA) software to measure the signal within individual hepatocytes after selecting equal areas of 20,000 pixels and plotted for each treatment group.

RNA and Quantitative PCR

Total RNA was isolated from the left lobe of the liver and was extracted according to the manufacturer's protocol (RNeasy Mini Kit, 74104; Qiagen, Hilden, Germany). A total of 2 μg RNA was converted to complementary DNA using the high-capacity complementary DNA reverse-transcription kit (4368813; Applied Biosystems, Foster City, CA). PCR was performed using SYBR Green PCR master mix (A25742; Applied Biosystems), and performed in a Quantstudio 6 Flex System (Applied Biosystems). The change in cycle threshold (delta CT) was normalized to 18S, and was expressed in fold change. The primer sequences were as follows: *Adora1* forward: 5'-TGTGACCACCACCCAGAGTA -3'; reverse: 5'-GCAGAGACTGGGACAAGGAG -3'; *Adora2a* forward: 5'-GAAGCAGATGGAGAGCCAAC -3'; reverse: 5'-GAGAGGAT GATGGCCAGGTA -3'; *Adora2b* forward: 5'-CCTTTGGCATTG GATTGACT -3'; reverse: 5'-AAAATGCCCACGATCATAGC -3'; *Adora3* forward: 5'-TCATACCGGAAGGAATGAGC -3'; reverse: 5'-AGCTTGACCACCCAGATGAC -3'; *Entpd1* forward: 5'-TAC CACCCCATCTGGTCATT-3'; reverse: 5'-GGACGTTTTGTTTTG GTTGGT -3'; *IL1β* forward: 5'-TCGCTCAGGGTCACAAGAAA-3'; reverse: 5'-CATCAGAGGCAAGGAGGAAAAC-3'; *TNFα* forward: 5'- AGGCTGCCCCGACTACGT-3'; reverse: 5'-GAC TTTCTCCTGGTATGAGATAGCAAA-3'; *Acaca* forward:5'-AGC CAGAAGGGACAGTAGAA-3'; reverse: 5'-CTCAGCCAAGCGG ATGTAAA-3'; *Hmgcr* forward: 5'-CTTGTGGAATGCCTTGT GATTG-3'; reverse: 5'-AGCCGAAGCAGCACATGAT-3'; *Hmgcs1* forward: 5'-GCCGTGAACTGGGTCGAA-3'; reverse: 5'-GCAT ATATAGCAATGTCTCCTGCAA-3'; *Srebp1a* forward: 5'-GGC CGAGATGTGCGAACT-3'; reverse: 5'-TTGTTGATGAGCTG GAGCATGT-3'; and *Srebp1c* forward: 5'-GGAGCCATG GATTGCACATT-3'; reverse: 5'-GGCCCGGGAAGTCACTGT-3'; *18S* forward: 5'-ACCTGGTTGATCCTGCCAGTAG-3'; reverse: 5'-TTAATGAGCCATTCGCAGTTTC-3'.

Liver Tissue Staining and CD73 Enzyme Histochemistry

Liver tissues from the left lobe were fixed with paraformaldehyde and paraffin-embedded, or flash-frozen using optimal cutting temperature (OCT) embedding medium. Paraffin-embedded tissues were cut in 10-μm sections and stained with hematoxylin and eosin (H&E). For immunohistochemistry, tissue sections were deparaffinized and rehydrated. Antigen was retrieved using HIER buffer pH 6.0 (TA-135-HBL; Thermo Fisher), and endogenous peroxidase was inhibited by 3% hydrogen peroxide. Tissues were blocked with 10% normal goat serum, and the primary antibody for the neutrophil marker Ly6G (2557; Abcam, Cambridge, United Kingdom) was incubated overnight at 4°C in blocking buffer. Secondary biotinylated anti-rat IgG was incubated for 1 hour at room temperature, followed by incubation with tertiary antibody (ABC Elite, PK-6100; Vector, Burlington, Ontario, Canada). Tissue sections were developed using 3,3'-diaminobenzidine substrate (TA-125-QHDX; Thermo Fisher), and counterstained with Harris hematoxylin. Images were analyzed using a 20× objective with the EVOS FL auto imaging system (Thermo Fisher). The average number of positive signals was quantified using ImageJ software (National Institutes of Health, Bethesda, MD) and plotted for each animal group. Frozen tissues were cut in 10-μm sections and stained by immunofluorescence. Briefly, frozen tissue sections were fixed in cold 10% normal buffered formalin (032-059; Fisher Scientific, Ottawa, Ontario, Canada), followed by cold acetone (A19-1; Fisher Scientific) for 10 minutes each. Tissues were blocked in 2% normal goat serum/2.5% bovine serum albumin/1× PBS for 1 hour at room temperature. Primary antibodies CD73 (clone TY/23, 550738; BD Pharmingen, San Jose, CA), K19-AF647 (ab192980; Abcam), K8/18 (clone 8592), and zonula occludens 1 (clone D6L1E, 13663; Cell Signaling) in blocking solution were incubated overnight at 4°C. Tissues were washed in 1× PBS, before adding the secondary antibodies anti-rat 488 (a11006; Thermo Fisher) and anti-rabbit 568 (a11079; Thermo Fisher) for 1 hour at room temperature. The nuclei were stained using 4',6-diamidino-2-phenylindole (D1306; Invitrogen, Carlsbad, CA). Images were analyzed at 40× oil objective using a Zeiss LSM 880 confocal microscope (Zeiss, Concord, NC). Frozen liver tissues sections of 10-μm thickness were fixed in 10% neutral buffered formalin for 5 minutes at 4°C. Enzyme histochemistry was performed using our published protocol.[13] Images were analyzed with a 20× objective using the EVOS-FL auto imaging system (Thermo Fisher).

Proteomic Analysis by Liquid Chromatography With Tandem Mass Spectrometry

Freshly isolated primary hepatocytes from 3 WT and 3 CD73-LKO mice were lysed using 8 mol/L urea. Protein lysates were digested with LysC-protease and trypsin. Peptide samples were cleaned using Pierce C18 spin columns (Thermo Fisher,), and then peptide quantitation was conducted. A total of 350 mg per sample was dried and labeled using the TMT 6-plex Isobaric Label Reagent Set (90061; Thermo Fisher). Label efficiency was evaluated and found to be >99% for all TMT channels. Samples were mixed, then subjected to fractionation into 96 fractions by high-pH, reversed-phase liquid chromatography. Samples were concatenated into 24 samples. Each sample (∼1 mg) was analyzed by liquid chromatography–tandem mass spectrometry using the QExactive HF (Thermo Fisher) for a total of 25 analyses. Proteins were identified and quantified using MaxQuant using a reviewed (∼18,000 proteins) mouse database appended with a common contaminants database. Core analysis of the liquid chromatography–tandem mass spectrometry data set was analyzed using Ingenuity Pathway Analysis (Qiagen) and filtered based on a log ($P = 1E^{-10}$) and an absolute z-score of 1.

Statistical Analysis

Data were analyzed using an unpaired t test or 2-way analysis of variance built in GraphPad Prism (San Diego, CA). Data are presented relative to WT or untreated controls. Error bars from all graphs indicate the SD for n ≥ 3 samples or independent experiments. P values are denoted within each respective figure panel. Outliers were tested based on the Grubb's test ($\alpha = .05$). The number of samples or independent experiments is indicated in the figure legends.

References

1. Younossi Z, Anstee QM, Marietti M, Hardy T, Henry L, Eslam M, George J, Bugianesi E. Global burden of NAFLD and NASH: trends, predictions, risk factors and prevention. Nat Rev Gastroenterol Hepatol 2018; 15:11–20.
2. Anstee QM, Reeves HL, Kotsiliti E, Govaere O, Heikenwalder M. From NASH to HCC: current concepts and future challenges. Nat Rev Gastroenterol Hepatol 2019;16:411–428.
3. Cotter TG, Rinella M. Nonalcoholic fatty liver disease 2020: the state of the disease. Gastroenterology 2020; 158:1851–1864.
4. Eslam M, Sanyal AJ, George J; International Consensus Panel. MAFLD: a consensus-driven proposed nomenclature for metabolic associated fatty liver disease. Gastroenterology 2020;158:1999–2014 e1.
5. Hyams DE, Isselbacher KJ. Prevention of fatty liver by administration of adenosine triphosphate. Nature 1964; 204:1196–1197.
6. Cortez-Pinto H, Chatham J, Chacko VP, Arnold C, Rashid A, Diehl AM. Alterations in liver ATP homeostasis in human nonalcoholic steatohepatitis: a pilot study. JAMA 1999;282:1659–1664.
7. Zimmermann H. 5'-Nucleotidase: molecular structure and functional aspects. Biochem J 1992;285:345–365.
8. Borea PA, Gessi S, Merighi S, Vincenzi F, Varani K. Pharmacology of adenosine receptors: the state of the art. Physiol Rev 2018;98:1591–1625.
9. Griffiths M, Beaumont N, Yao SY, Sundaram M, Boumah CE, Davies A, Kwong FY, Coe I, Cass CE,

Young JD, Baldwin SA. Cloning of a human nucleoside transporter implicated in the cellular uptake of adenosine and chemotherapeutic drugs. Nat Med 1997;3:89–93.

10. Spychala J, Datta NS, Takabayashi K, Datta M, Fox IH, Gribbin T, Mitchell BS. Cloning of human adenosine kinase cDNA: sequence similarity to microbial ribokinases and fructokinases. Proc Natl Acad Sci U S A 1996; 93:1232–1237.

11. Colgan SP, Eltzschig HK, Eckle T, Thompson LF. Physiological roles for ecto-5'-nucleotidase (CD73). Purinergic Signal 2006;2:351–360.

12. Minor M, Alcedo KP, Battaglia RA, Snider NT. Cell type- and tissue-specific functions of ecto-5'-nucleotidase (CD73). Am J Physiol Cell Physiol 2019; 317:C1079–C1092.

13. Snider NT, Griggs NW, Singla A, Moons DS, Weerasinghe SV, Lok AS, Ruan C, Burant CF, Conjeevaram HS, Omary MB. CD73 (ecto-5'-nucleotidase) hepatocyte levels differ across mouse strains and contribute to Mallory-Denk body formation. Hepatology 2013;58:1790–1800.

14. Snider NT, Altshuler PJ, Wan S, Welling TH, Cavalcoli J, Omary MB. Alternative splicing of human NT5E in cirrhosis and hepatocellular carcinoma produces a negative regulator of ecto-5'-nucleotidase (CD73). Mol Biol Cell 2014;25:4024–4033.

15. Alcedo KP, Guerrero A, Basrur V, Fu D, Richardson ML, McLane JS, Tsou CC, Nesvizhskii AI, Welling TH, Lebrilla CB, Otey CA, Kim HJ, Omary MB, Snider NT. Tumor-selective altered glycosylation and functional attenuation of CD73 in human hepatocellular carcinoma. Hepatol Commun 2019;3:1400–1414.

16. Ben-Moshe S, Shapira Y, Moor AE, Manco R, Veg T, Bahar Halpern K, Itzkovitz S. Spatial sorting enables comprehensive characterization of liver zonation. Nat Metab 2019;1:899–911.

17. Moor AE, Harnik Y, Ben-Moshe S, Massasa EE, Rozenberg M, Eilam R, Bahar Halpern K, Itzkovitz S. Spatial reconstruction of single enterocytes uncovers broad zonation along the intestinal villus axis. Cell 2018; 175:1156–1167 e15.

18. Broeker KAE, Fuchs MAA, Schrankl J, Kurt B, Nolan KA, Wenger RH, Kramann R, Wagner C, Kurtz A. Different subpopulations of kidney interstitial cells produce erythropoietin and factors supporting tissue oxygenation in response to hypoxia in vivo. Kidney Int 2020;98:918–931.

19. Synnestvedt K, Furuta GT, Comerford KM, Louis N, Karhausen J, Eltzschig HK, Hansen KR, Thompson LF, Colgan SP. Ecto-5'-nucleotidase (CD73) regulation by hypoxia-inducible factor-1 mediates permeability changes in intestinal epithelia. J Clin Invest 2002; 110:993–1002.

20. Tak E, Jung DH, Kim SH, Park GC, Jun DY, Lee J, Jung BH, Kirchner VA, Hwang S, Song GW, Lee SG. Protective role of hypoxia-inducible factor-1alpha-dependent CD39 and CD73 in fulminant acute liver failure. Toxicol Appl Pharmacol 2017;314:72–81.

21. Hart ML, Much C, Gorzolla IC, Schittenhelm J, Kloor D, Stahl GL, Eltzschig HK. Extracellular adenosine production by ecto-5'-nucleotidase protects during murine hepatic ischemic preconditioning. Gastroenterology 2008;135:1739–1750 e3.

22. Thompson LF, Eltzschig HK, Ibla JC, Van De Wiele CJ, Resta R, Morote-Garcia JC, Colgan SP. Crucial role for ecto-5'-nucleotidase (CD73) in vascular leakage during hypoxia. J Exp Med 2004;200:1395–1405.

23. Gebhardt R. Metabolic zonation of the liver: regulation and implications for liver function. Pharmacol Ther 1992; 53:275–354.

24. Hall Z, Bond NJ, Ashmore T, Sanders F, Ament Z, Wang X, Murray AJ, Bellafante E, Virtue S, Vidal-Puig A, Allison M, Davies SE, Koulman A, Vacca M, Griffin JL. Lipid zonation and phospholipid remodeling in nonalcoholic fatty liver disease. Hepatology 2017;65:1165–1180.

25. Koupenova M, Ravid K. Adenosine, adenosine receptors and their role in glucose homeostasis and lipid metabolism. J Cell Physiol 2013;228:1703–1712.

26. Allard B, Allard D, Buisseret L, Stagg J. The adenosine pathway in immuno-oncology. Nat Rev Clin Oncol 2020; 17:611–629.

27. Willingham SB, Criner G, Hill C, Hu S, Rudnick JA, Daine-Matsuoka B, Hsieh J, Mashhedi H, Hotson AN, Brody J, Marron T, Piccione E, Buggy JJ, Mahabhashyam S, Jones WB, Mobasher M, Miller RA. Characterization and phase 1 trial of a B cell activating anti-CD73 antibody for the immunotherapy of COVID-19. medRxiv 2020:2020. 09.10.20191486.

28. Tabula Muris Consortium, Overall coordination, Logistical coordination, Organ collection and processing, Library preparation and sequencing, Computational data analysis, Cell type annotation, Writing group; Supplemental text writing group, Principal investigators. Single-cell transcriptomics of 20 mouse organs creates a Tabula Muris. Nature 2018;562:367–372.

29. Ang CH, Hsu SH, Guo F, Tan CT, Yu VC, Visvader JE, Chow PKH, Fu NY. Lgr5(+) pericentral hepatocytes are self-maintained in normal liver regeneration and susceptible to hepatocarcinogenesis. Proc Natl Acad Sci U S A 2019;116:19530–19540.

30. Wang B, Zhao L, Fish M, Logan CY, Nusse R. Self-renewing diploid Axin2(+) cells fuel homeostatic renewal of the liver. Nature 2015;524:180–185.

31. Gwinn DM, Shackelford DB, Egan DF, Mihaylova MM, Mery A, Vasquez DS, Turk BE, Shaw RJ. AMPK phosphorylation of raptor mediates a metabolic checkpoint. Mol Cell 2008;30:214–226.

32. Pastor-Anglada M, Perez-Torras S. Who is who in adenosine transport. Front Pharmacol 2018;9:627.

33. Cai Y, Li H, Liu M, Pei Y, Zheng J, Zhou J, Luo X, Huang W, Ma L, Yang Q, Guo S, Xiao X, Li Q, Zeng T, Meng F, Francis H, Glaser S, Chen L, Huo Y, Alpini G, Wu C. Disruption of adenosine 2A receptor exacerbates NAFLD through increasing inflammatory responses and SREBP1c activity. Hepatology 2018;68:48–61.

34. Garcia D, Hellberg K, Chaix A, Wallace M, Herzig S, Badur MG, Lin T, Shokhirev MN, Pinto AFM, Ross DS, Saghatelian A, Panda S, Dow LE, Metallo CM, Shaw RJ. Genetic liver-specific AMPK activation protects against diet-induced obesity and NAFLD. Cell Rep 2019; 26:192–208 e6.

35. Volmer JB, Thompson LF, Blackburn MR. Ecto-5'-nucleotidase (CD73)-mediated adenosine production is tissue protective in a model of bleomycin-induced lung injury. J Immunol 2006;176:4449–4458.

36. Grenz A, Zhang H, Eckle T, Mittelbronn M, Wehrmann M, Kohle C, Kloor D, Thompson LF, Osswald H, Eltzschig HK. Protective role of ecto-5'-nucleotidase (CD73) in renal ischemia. J Am Soc Nephrol 2007; 18:833–845.

37. Gehrke N, Schattenberg JM. Metabolic inflammation-a role for hepatic inflammatory pathways as drivers of comorbidities in nonalcoholic fatty liver disease? Gastroenterology 2020;158:1929–1947 e6.

38. Peng Z, Borea PA, Varani K, Wilder T, Yee H, Chiriboga L, Blackburn MR, Azzena G, Resta G, Cronstein BN. Adenosine signaling contributes to ethanol-induced fatty liver in mice. J Clin Invest 2009; 119:582–594.

39. Peng Z, Fernandez P, Wilder T, Yee H, Chiriboga L, Chan ES, Cronstein BN. Ecto-5'-nucleotidase (CD73)-mediated extracellular adenosine production plays a critical role in hepatic fibrosis. FASEB J 2008; 22:2263–2272.

40. Shih YV, Liu M, Kwon SK, Iida M, Gong Y, Sangaj N, Varghese S. Dysregulation of ectonucleotidase-mediated extracellular adenosine during post-menopausal bone loss. Sci Adv 2019;5:eaax1387.

41. Borgus JR, Puthongkham P, Venton BJ. Complex sex and estrous cycle differences in spontaneous transient adenosine. J Neurochem 2020;153:216–229.

42. Mitrović N, Zarić M, Drakulić D, Martinović J, Stanojlović M, Sévigny J, Horvat A, Nedeljković N, Grković I. 17β-Estradiol upregulates ecto-5'-nucleotidase (CD73) in hippocampal synaptosomes of female rats through action mediated by estrogen receptor-α and -β. Neuroscience 2016;324:286–296.

43. Wang Y, Copeland J, Shin M, Chang Y, Venton BJ. CD73 or CD39 deletion reveals different mechanisms of formation for spontaneous and mechanically stimulated adenosine and sex specific compensations in ATP degradation. ACS Chem Neurosci 2020; 11:919–928.

44. Cotter DG, Ercal B, Huang X, Leid JM, d'Avignon DA, Graham MJ, Dietzen DJ, Brunt EM, Patti GJ, Crawford PA. Ketogenesis prevents diet-induced fatty liver injury and hyperglycemia. J Clin Invest 2014; 124:5175–5190.

45. Timilshina M, You Z, Lacher SM, Acharya S, Jiang L, Kang Y, Kim JA, Chang HW, Kim KJ, Park B, Song JH, Ko HJ, Park YY, Ma MJ, Nepal MR, Jeong TC, Chung Y, Waisman A, Chang JH. Activation of mevalonate pathway via LKB1 is essential for stability of Treg cells. Cell Rep 2019;27:2948–2961 e7.

46. Mauvais-Jarvis F, Bairey Merz N, Barnes PJ, Brinton RD, Carrero JJ, DeMeo DL, De Vries GJ, Epperson CN, Govindan R, Klein SL, Lonardo A, Maki PM, McCullough LD, Regitz-Zagrosek V, Regensteiner JG, Rubin JB, Sandberg K, Suzuki A. Sex and gender: modifiers of health, disease, and medicine. Lancet 2020; 396:565–582.

47. Heron M. Deaths: leading causes for 2017. Natl Vital Stat Rep 2019;68:1–77.

48. Vilar-Gomez E, Calzadilla-Bertot L, Wai-Sun Wong V, Castellanos M, Aller-de la Fuente R, Metwally M, Eslam M, Gonzalez-Fabian L, Alvarez-Quinones Sanz M, Conde-Martin AF, De Boer B, McLeod D, Hung Chan AW, Chalasani N, George J, Adams LA, Romero-Gomez M. Fibrosis severity as a determinant of cause-specific mortality in patients with advanced nonalcoholic fatty liver disease: a multi-national cohort study. Gastroenterology 2018;155:443–457 e17.

49. Lonardo A, Nascimbeni F, Ballestri S, Fairweather D, Win S, Than TA, Abdelmalek MF, Suzuki A. Sex differences in nonalcoholic fatty liver disease: state of the art and identification of research gaps. Hepatology 2019; 70:1457–1469.

50. Norheim F, Hui ST, Kulahcioglu E, Mehrabian M, Cantor RM, Pan C, Parks BW, Lusis AJ. Genetic and hormonal control of hepatic steatosis in female and male mice. J Lipid Res 2017;58:178–187.

51. Norheim F, Bjellaas T, Hui ST, Chella Krishnan K, Lee J, Gupta S, Pan C, Hasin-Brumshtein Y, Parks BW, Li DY, Bui HH, Mosier M, Wu Y, Huertas-Vazquez A, Hazen SL, Gundersen TE, Mehrabian M, Tang WHW, Hevener AL, Drevon CA, Lusis AJ. Genetic, dietary, and sex-specific regulation of hepatic ceramides and the relationship between hepatic ceramides and IR. J Lipid Res 2018; 59:1164–1174.

52. Chella Krishnan K, Sabir S, Shum M, Meng Y, Acin-Perez R, Lang JM, Floyd RR, Vergnes L, Seldin MM, Fuqua BK, Jayasekera DW, Nand SK, Anum DC, Pan C, Stiles L, Peterfy M, Reue K, Liesa M, Lusis AJ. Sex-specific metabolic functions of adipose Lipocalin-2. Mol Metab 2019;30:30–47.

53. Kurt Z, Barrere-Cain R, LaGuardia J, Mehrabian M, Pan C, Hui ST, Norheim F, Zhou Z, Hasin Y, Lusis AJ, Yang X. Tissue-specific pathways and networks underlying sexual dimorphism in non-alcoholic fatty liver disease. Biol Sex Differ 2018;9:46.

54. Norheim F, Hasin-Brumshtein Y, Vergnes L, Chella Krishnan K, Pan C, Seldin MM, Hui ST, Mehrabian M, Zhou Z, Gupta S, Parks BW, Walch A, Reue K, Hofmann SM, Arnold AP, Lusis AJ. Gene-by-sex interactions in mitochondrial functions and cardio-metabolic traits. Cell Metab 2019;29:932–949 e4.

55. Peralta C, Bartrons R, Serafin A, Blazquez C, Guzman M, Prats N, Xaus C, Cutillas B, Gelpi E, Rosello-Catafau J. Adenosine monophosphate-activated protein kinase mediates the protective effects of ischemic pre-conditioning on hepatic ischemia-reperfusion injury in the rat. Hepatology 2001;34:1164–1173.

56. Mulligan JD, Gonzalez AA, Kumar R, Davis AJ, Saupe KW. Aging elevates basal adenosine monophosphate-activated protein kinase (AMPK) activity and eliminates hypoxic activation of AMPK in mouse liver. J Gerontol A Biol Sci Med Sci 2005;60:21–27.

57. Hwang AB, Ryu EA, Artan M, Chang HW, Kabir MH, Nam HJ, Lee D, Yang JS, Kim S, Mair WB, Lee C, Lee SS, Lee SJ. Feedback regulation via AMPK and HIF-1 mediates ROS-dependent longevity in Caenorhabditis

elegans. Proc Natl Acad Sci U S A 2014; 111:E4458–E4467.

58. Rabinovitch RC, Samborska B, Faubert B, Ma EH, Gravel SP, Andrzejewski S, Raissi TC, Pause A, St-Pierre J, Jones RG. AMPK maintains cellular metabolic homeostasis through regulation of mitochondrial reactive oxygen species. Cell Rep 2017;21:1–9.

59. Burnstock G, Vaughn B, Robson SC. Purinergic signalling in the liver in health and disease. Purinergic Signal 2014;10:51–70.

60. Hotamisligil GS. Inflammation, metaflammation and immunometabolic disorders. Nature 2017;542:177–185.

61. Ohta A, Sitkovsky M. Role of G-protein-coupled adenosine receptors in downregulation of inflammation and protection from tissue damage. Nature 2001; 414:916–920.

62. Chouker A, Thiel M, Lukashev D, Ward JM, Kaufmann I, Apasov S, Sitkovsky MV, Ohta A. Critical role of hypoxia and A2A adenosine receptors in liver tissue-protecting physiological anti-inflammatory pathway. Mol Med 2008;14:116–123.

63. Cordero-Herrera I, Kozyra M, Zhuge Z, McCann Haworth S, Moretti C, Peleli M, Caldeira-Dias M, Jahandideh A, Huirong H, Cruz JC, Kleschyov AL, Montenegro MF, Ingelman-Sundberg M, Weitzberg E, Lundberg JO, Carlstrom M. AMP-activated protein kinase activation and NADPH oxidase inhibition by inorganic nitrate and nitrite prevent liver steatosis. Proc Natl Acad Sci U S A 2019;116:217–226.

64. Hoxhaj G, Hughes-Hallett J, Timson RC, Ilagan E, Yuan M, Asara JM, Ben-Sahra I, Manning BD. The mTORC1 signaling network senses changes in cellular purine nucleotide levels. Cell Rep 2017;21:1331–1346.

65. Postic C, Shiota M, Niswender KD, Jetton TL, Chen Y, Moates JM, Shelton KD, Lindner J, Cherrington AD, Magnuson MA. Dual roles for glucokinase in glucose homeostasis as determined by liver and pancreatic beta cell-specific gene knock-outs using Cre recombinase. J Biol Chem 1999;274:305–315.

Correspondence
Address correspondence to: Natasha Snider, PhD, Department of Cell Biology and Physiology, University of North Carolina–Chapel Hill, 5340C MBRB, 111 Mason Farm Road, Chapel Hill, North Carolina 27516. e-mail: ntsnider@med.unc.edu; fax: (919) 966-6927.

CRediT Authorship Contributions
  Karel Alcedo (Conceptualization: Equal; Data curation: Lead; Formal analysis: Lead; Funding acquisition: Supporting; Investigation: Lead; Methodology: Lead; Supervision: Equal; Writing – original draft: Equal; Writing – review & editing: Equal)
  Morgan Rouse (Data curation: Supporting; Investigation: Supporting; Methodology: Supporting; Writing – review & editing: Supporting)
  Gloria Jung (Data curation: Supporting; Investigation: Supporting; Writing – review & editing: Supporting)
  Dong Fu (Data curation: Supporting; Investigation: Supporting; Writing – review & editing: Supporting)
  Marquet Minor (Data curation: Supporting; Investigation: Supporting; Writing – review & editing: Supporting)
  Helen Willcockson (Data curation: Supporting; Formal analysis: Supporting; Investigation: Equal; Methodology: Supporting)
  Kevin Greene (Formal analysis: Equal; Methodology: Equal)
  Natasha Snider, PhD (Conceptualization: Lead; Data curation: Supporting; Formal analysis: Equal; Funding acquisition: Lead; Investigation: Supporting; Methodology: Supporting; Project administration: Lead; Resources: Lead; Supervision: Lead; Validation: Lead; Visualization: Lead; Writing – original draft: Equal; Writing – review & editing: Lead)

Conflicts of interest
The authors disclose no conflicts.